Hashemi et al., *BioImpacts*, 2023, 13(4), 275-287
doi: 10.34172/bi.2023.26317
http://bi.tbzmed.ac.ir/

Preparation and evaluation of a polycaprolactone/chitosan/propolis fibrous nanocomposite scaffold as a tissue engineering skin substitute

Seyedeh-Sara Hashemi[1,2], Ali-Akbar Mohammadi[1,3], Seyedeh-Somayeh Rajabi[4], Parisa Sanati[1,5], Alireza Rafati[6], Mehdi Kian[2,7*], Zahra Zarei[3*]

[1]Burn and Wound Healing Research Center, Shiraz University of Medical Sciences, Shiraz, Iran
[2]Department of Comparative Biomedical Sciences, School of Advanced Medical Sciences and Technologies, Shiraz University of Medical Sciences, Shiraz, Fars, Iran
[3]Division of Plastic and Reconstructive Surgery, Department of Surgery, Shiraz University of Medical Sciences, Shiraz, Fars, Iran
[4]Department of Tissue Engineering, School of Medicine, Fasa University of Medical Sciences, Fasa, Iran
[5]Iran National Elite Foundation, Tehran, Iran
[6]Division of Pharmacology and Pharmaceutical Chemistry, Sarvestan Branch, Islamic Azad University, Sarvestan, Fars, Iran
[7]Student Research Committee, Shiraz University of Medical Sciences, Shiraz, Fars, Iran

Article Info

Article Type:
Original Article

Article History:
Received: 5 Apr. 2022
Revised: 5 Sep. 2022
Accepted: 12 Sep. 2022
ePublished: 11 June 2023

Keywords:
Skin substitutes
Polycaprolactone
Chitosan
Propolis
Nanofibers
Wound healing

Abstract

Introduction: Recently, the application of nanofibrous mats for dressing skin wounds has received great attention. In this study, we aimed to fabricate and characterize an electrospun nanofibrous mat containing polycaprolactone (PCL), chitosan (CTS), and propolis for use as a tissue-engineered skin substitute.

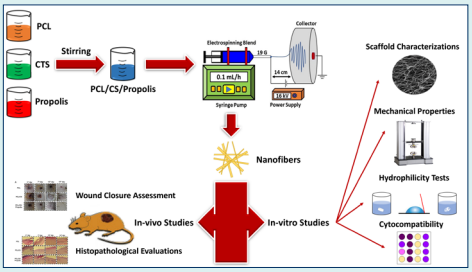

Methods: Raw propolis was extracted, and its phenolic and flavonoid contents were measured. The physiochemical and biological properties of the fabricated mats, including PCL, PCL/CTS, and PCL/CTS/Propolis were evaluated by scanning electron microscopy (SEM), atomic force microscopy (AFM), mechanical analysis, swelling and degradation behaviors, contact angle measurement, cell attachment, DAPI staining, and MTT assay. On the other hand, the drug release pattern of propolis from the PCL/CTS/Propolis scaffold was determined. A deep second-degree burn wound model was induced in rats to investigate wound healing using macroscopical and histopathological evaluations.

Results: The results revealed that the propolis extract contained high amounts of phenolic and flavonoid compounds. The fabricated scaffold had suitable physicochemical and mechanical properties. Uniform, bead-free, and well-branched fibers were observed in SEM images of mats. AFM analysis indicated that the addition of CTS and propolis to PCL elevated the surface roughness. MTT results revealed that the electrospun PCL/CTS/Propolis mat was biocompatible. The presence of fibroblast cells on the PCL/CTS/Propolis mats was confirmed by DAPI staining and SEM images. Also, propolis was sustainably released from the PCL/CTS/Propolis mat. The animal study revealed that addition of propolis significantly improved wound healing.

Conclusion: The nanofibrous PCL/CTS/Propolis mat can be applied as a tissue-engineered skin substitute for healing cutaneous wounds, such as burn wounds.

Introduction

Skin is an important organ of the body that has various essential vital functions, including the sensation of physical and chemical stimuli; thermoregulation; maintenance of underlying tissues moisture; elimination of excess fluids, ions, and biological byproducts; synthesis and storage of numerous bio-compounds (e.g., pigments, vitamin D, and keratins); and especially a protective barrier agent against adverse environmental agents. Skin can undergo severe or chronic injuries by trauma, pressure sores, burns, as well as some diseases such as diabetes that result in impairment or even inability of the skin functions. Hence, regeneration

*Corresponding authors: Mehdi Kian, Email: mehdi.kian@live.com; Zahra Zarei, Email: zarei2218@gmail.com

of the damaged skin is very important.[1]

Tissue engineering is a novel biotechnology used to regenerate and reconstruct damaged or lost tissues such as the skin. Designing biological mats is one of the therapeutic strategies in this field for providing a 3D micro-environment analogous to the native tissues of the body.[2] Recently, nanofibrous mats have gained attention to be applicated for healing skin wounds. These nano-products mimic the extracellular matrix by providing a complex network with high porosity, leading to acceleration of the wound healing process. In addition to biocompatibility and biodegradability, they can also maintain wound humidity, inhibit wound contraction, and prevent bacterial penetration to the wound.[3,4]

Hitherto, many nanofibrous mats have been fabricated using the electrospinning technique to be applicated as a skin wound dressing scaffold. Commonly, synthetic and natural polymeric biomaterials are blended to achieve favorable and durable nanofibrous mats. Synthetic polymers have proper mechanical and biodegradation characteristics that aid the growth of new tissue. In addition to inexpensiveness, they can also be solved in a broad range of solvents. On the other hand, natural biopolymers have good biocompatibility, biodegradability, and hydrophilicity.[3] Polycaprolactone (PCL) is a commonly used synthetic semi-crystalline polymer in skin bioengineering. In addition to its low melting point (Tm - 60°C) and easy ductility at low temperatures, PCL has desirable mechanical properties and biocompatibility.[5] Due to its good permeability to various drugs and degradability properties, PCL is an appropriate biomaterial to be applicated for controlled drug delivery release.[6,7] Chitosan (CTS) is a linear natural polymer with acetyl and amine branches and the most common chitin derivative found in aquatic shells such as shrimp, crab, and mushroom walls. Because of its structural resemblance to glycosaminoglycan, CTS is hydrophilic. CTS possesses bacteriostatic and bactericidal activities as a result of its cationic nature.[8,9] Besides, because of the CTS 3D structure, its network and porous nanofiber mat can absorb the pus and blood wetness and has a good oxygen permeability in the area. Also, owing to its biodegradability, biocompatibility, swelling, as well as mechanical strength properties, CTS is widely applicated in controlled delivery systems.[10]

Studies have shown that using an electrospinning approach to generate a PCL/CTS fibrous mat improves the wound healing. The addition of PCL to CTS increases the mechanical characteristics of the network while lowering its hydrophilicity. The ability to preserve the physical integrity of the three-component scaffold network in the environment (such as the wound environment, etc.) improves when hydrophilicity is reduced. In these types of scaffolds, the fibroblast cells grow well, flatten, and adhere to the nanofibers properly.[11-13]

Propolis is a hydrophobic complex natural substance produced by honeybees made up of secretions of plants. Currently, more than 300 compounds have been found in different kinds of propolis.[14] Raw propolis consists of 50% resin, a combination of flavonoids and phenolic acids, aromatic acids, and related esters, aldehydes and ketones, which is considered the polyphenolic part.[15-17] Foam, essential oils, pollen, and other organic substances are also present (amino acids, steroids, alcohol, polysaccharides, hydrocarbon, hydroxybenzene, and water).[16,17] Propolis possesses antiseptic, antibacterial, antiviral, anti-inflammatory, anti-cancer, and antioxidant properties.[15-17] Propolis can accelerate the healing of skin wounds by enhancing activation and proliferation of the skin cells, reducing inflammation, and scavenging free radicals at the wound site.[15] It is well-tolerated, with only a few cases of allergy and no toxicity.[15,18] Topical administration of propolis stimulates the accumulation of sulfated glycosaminoglycans that are essential for tissue granulation in the wound bed, tissue growth, and wound closure. Additionally, propolis elevates the structural modification of Chondroitin/Dermatan sulfate that helps to bind growth factors that participate in tissue repair to them.[19] Propolis can also neutralize free radicals in the skin.[20]

In this study, a nanofibrous mat composed of PCL, CTS, and propolis was fabricated for promoting wound healing. The produced mat was expected to not only have suitable physiochemical properties and good biocompatibility, but also accelerate the healing process.

Material and Methods

Materials

PCL (Mw=80 kDa), CTS (Mw=310-375 kDa, >75% deacetylate), DAPI powder, glacial acetic acid, T25 and T75 cell culture flasks, 96-well plates, ethanol, Whatman filter paper No. 1, Folin–Ciocalteu Reagent, sodium carbonate, methanol, gallic acid standard, quercetin standard, ethanol, potassium acetate, aluminum chloride, and Dulbecco's modified Eagle's medium/F12 (DMEM) were purchased from Sigma Aldrich (USA). Micro-culture thiazolyl blue tetrazolium bromide (MTT) was purchased from Invitrogen (USA). Dimethyl sulfoxide (DMSO), phosphate-buffered saline (PBS), streptomycin, penicillin, and fetal bovine serum (FBS) were obtained from Life Technologies Inc (USA). Raw propolis was obtained from Yas Company (Iran).

Propolis extraction

After freeze-drying, 4 g of raw propolis was pounded in a mortar until a homogeneous powder was obtained. Then, the obtained powder was mixed with 100 mL of 70% ethanol and shaken for 48 hours at room temperature. The unsolved materials in the prepared solution were filtered by Whatman filter paper No. 1. Next, the solution was concentrated using a rotary evaporator (Heidolph, Laborota 4003, Germany) under the vacuum condition

at 40°C. After the remained solution reached a volume of 5 mL, it was transferred to a 15 mL Falcon tube and centrifuged for 5 minutes at 3000 rpm. The supernatant was separated and dried in a freeze-dry machine (LyoLab 10, Antech Group Inc., China) to completely remove the solvent; then, we stored it at -20°C until usage.

Measurement of total phenolic content in the propolis extract

The amount of total phenolic content was measured by Folin-Ciocalteu colorimetric method using Gallic acid as a standard based on the Escriche and Juan-Borras' method with some modifications.[21] First, concentrations of 6.25, 12.5, 25, 50, 100, and 200 mg/mL were prepared by dissolving the Gallic acid standard in methanol. Then, each concentration was added to 5 ml of Folin–Ciocalteu reagent and 4 mL of 1 M sodium carbonate. The tubes containing the prepared solutions were placed in a water bath for 20 minutes at 40°C temperature; then, to terminate the reaction, we quickly placed the tubes on crushed ice. In order to determine the Gallic acid standard curve, we read the absorbance of the samples from low to high concentration by a spectrophotometer (Model: T–90+, PG instrument, UK) at 756 nm wavelength. Using UV-Vis software, we drew the standard curves of Gallic acid and its equation was presented (equation 1). To determine the total phenols in propolis, we dissolved 2.5 mg of the prepared extract in 10 mL of 95% methanol to prepare the stock solution. Then, the amount of total phenol in the 0.5 mL propolis stock solution was determined, using the described method and the Gallic acid standard calibration curve. Finally, the amount of total phenol per gram of propolis was calculated (each test was done three times).

$$Abs = K1*(Conc) + K0 \quad \text{Eq. (1)}$$

K0: 0.00706, K1: 0.00469, R^2: 0.9998.

Measurement of total flavonoid content in the propolis extract

The aluminum chloride colorimetric assay was used to measure the total flavonoids in the propolis extract based on Chang and colleagues' method with a little modification.[22] Quercetin was used to make the calibration curve. Briefly, 10 mg of Quercetin was dissolved in 80% ethanol and then diluted to 25, 50, and 100 µg/mL. The diluted solutions (0.5 ml) were on an individual basis mixed with 1.5 mL of 95% ethanol, 0.1 mL of 10% aluminum chloride, 0.1 mL of 1M potassium acetate, and 2.8 mL of distilled water. The prepared mixture was then incubated at 25°C for 30 minutes and then its absorbance was measured at 415 nm with a spectrophotometer (T90+, PG instrument, UK). The amount of 10% aluminum chloride was substituted by the same amount of distilled water in the blank. UV-Vis software package was accustomed to drawing the calibration curves of quercetin and its equation was obtained (equation 2). Similarly, 0.5 mL of propolis extract stock solution was reacted with aluminum chloride to determine the flavonoid content using quercetin standard activity curve (each test was done three times).

$$Abs = K1*(Conc) + K0 \quad \text{Eq. (2)}$$

K0: -0.00953, K1: 0.02922, R^2: 0.9998

Preparation of fibrous mats

The acetic acid 90% solution was used to separately prepare 18% w/v PCL, 0/4% w/v CTS and 0.27% w/v propolis solutions under magnetic stirring. PCL/CTS and PCL/CTS/Propolis blends were created by mixing the base solutions in a 3:1 and 3:1:1 ratio, respectively. Based on pilot tests, electrospinning parameters were set to 0.1 mL/h injection rate, 19-gauge metallic needle, 14 cm distance between nozzle and aluminum collector, and voltages of 16 kV.

Scanning electron microscopy (SEM) of nanofiber mat and ImageJ analysis

The morphological structure of the fabricated mats was evaluated by SEM (model Vega3, Tescan, Czech Republic). The micrographs from each mat were analyzed by ImageJ software (version 1.51w, NIH, USA), using the DiameterJ plugin based on Hotaling and colleagues'[23] method with some modifications. Briefly, SEM images of the mats were segmented, and then five segmented images from each mat that had a proper quality were analyzed to measure the fiber diameter frequency, average diameter of the fibers as well as the area of the pores, porosity percent, number of pores, and intersection density of the electrospun fibrous mats.

Atomic force microscopy (AFM)

The surface roughness of the fabricated mats was evaluated by AFM (model ARA AFM, ARA RESEARCH Co., Iran) in contact mode. The surface roughness was obtained by dragging the tip along the surface of PCL, PCL/CTS, and PCL/CTS/ propolis mats.

Fourier-transform infrared spectroscopy (FTIR) of the mats

The chemical composition of the fabricated mats was evaluated using FTIR spectroscopy. FTIR spectra of the PCL, PCL/CTS, and PCL/CTS/ propolis mats were obtained in the 400-4000 cm^{-1} range, using diffuse reflectance mode over 64 scans with a resolution of 2 cm^{-1} (model Paragon 1000, Perkin-Elmer, USA).

Mechanical properties of mats

A tabletop micro-tester was used to determine the mechanical properties of electrospun nanofibrous mats (Instron instrument, USA). Strip-shaped (10×10 mm) samples were cut and tested at a crosshead speed of 0.5 mm/min (ASTM D882 standard). For each group of electrospun nanofibrous mats, at least three samples were

tested. Ultimate tensile strength (UTS) and the percentage elongation at break were calculated based on the generated stress-strain curves.

Contact angle

The hydrophilicity of the mats was assessed using the sessile drop method, which measured the water contact angle (SSC, DC318P color video camera, Japan). Three drops of distilled water were placed on each mat before it was placed on a support holder. After placement, the images of the droplets were captured, and the water contact angle was measured using ImageJ software (version 1.51w, NIH, USA).

Fluid uptake capacity

Fabricated mats were cut into square pieces (10×10 mm) and weighted. Then, the dry samples were immersed in PBS solution (pH 7.4) before being incubated at 37°C for 1, 6, 12, and 24 hours. The samples were weighed after the surface water was removed. The swelling ratio was then calculated using equation 3:

$$Swelling\ ratio\ (\%) = (W_s - W_d)/\ W_d \times 100 \quad \text{Eq. (3)}$$

Where W_s and W_0 are the final swollen weight and initial dry weight, respectively.

Degradation study of the mats

The mats were cut into discs with a radius of 20 mm and weighed to determine the initial dry mass (Wi). After that, the dried films were immersed into 50 mL capped Falcon tubes containing 25 mL of PBS and placed inside a shaker oven for 21 days at 37°C. Thereafter, the solution was filtered through Whatman filter paper (No. 1) to recover the remaining undissolved films. The remaining film pieces were placed in the vacuum oven at 70°C for 2 hours and then weighed to determine the final dry mass of the mats. The percentage of the remaining weight was calculated according to the following equation:

$$Remaining\ weight\ (\%) = W_r/\ W_i \times 100 \quad \text{Eq. (4)}$$

Where W_r and W_i are the remaining and final weights, respectively.

In vitro release of propolis from the PCL/CTS/Propolis mat

In vitro release of propolis from the PCL/CTS/Propolis mat was carried out by immersing the three 0.5×0.5 cm square samples in 3 mL of saline solution and incubating at 37°C using a shaker incubator (Model KM11, Fan Azma Gostar, Iran) set at 40 RPM. At several time intervals, the medium was collected and replenished with fresh medium to maintain the sink conditions. The drug release was measured by the optical density using a UV spectrophotometer (Model: T–90+, PG instrument, UK) at 326 nm wavelengths, and finally the cumulative percentage of propolis release was calculated.

Cell culture

Human dermal fibroblasts (HDFs) were cultured in a DMEM medium. A 10% FBS and 1% penicillin-streptomycin (100 units/mL in 100 g/mL) solution were provided in an incubator (Termo Fisher Scientific, USA) with a humidified atmosphere containing 5% CO_2 at 37°C. T-25 and T-75 tissue culture flasks were cultured with adherent monolayer cultures of the cells.

in vitro cell viability

MTT assay was performed to evaluate the cytotoxicity of the mats. For this purpose, mats were punched, and after sterilization of both sides of them under UV irradiation for 1 hour, they were placed into the 96-well plates. Subsequently, 1×10^3 HDFs were seeded in each well and incubated at 37°C. After 24, 48, and 72 hours, the culture plates were taken out from the incubator, and 20 µL of MTT solution was added to each well and incubated for 4 hours. The solutions were then removed, and DMSO solution was added before incubating for 30 minutes at 37°C. An ELISA reader (BioTek Inc., USA) was used to read the UV absorbance spectra at 570 nm.

In vitro cell attachment

Like the cell viability evaluation method, the mats were punched and after sterilization of both sides of them under UV irradiation for 1 hour, they were placed into the 96-well plates. Subsequently, 1×10^4 HDFs were seeded to each well and incubated at 37°C. After 24 hours, a total of 100 µL of glutaraldehyde (2.5%) was then added to the wells, and the cells were fixed on the mat and stored for 4 hours in the refrigerator. The mats were then washed with distilled water, then dehydrated with ethanol alcohols (concentrations of 25%, 50%, 75%, and 100%), and finally evaluated by SEM.

DAPI staining

In 12-well plates, the mats were placed and 1×10^4 HDFs were seeded into the wells. Then, the plates were incubated in a CO_2 incubator for 24 hours before the mats were fixed in formalin solution (4%) in the incubator for 30 minutes. Then, each well received 0.1% triton X-100 and was incubated for 5 minutes at 37°C. The mats were then washed twice with PBS solution before 100 l DAPI stain (1/1000 diluted) was applied and incubated at 37°C for 30 minutes. A fluorescent microscope was used to photograph the samples after they had been washed three times with PBS (MF53, OLYMPUS, Germany).

Animal model study

To assess the biocompatibility of the mats, we used a burn wound model. Sixty Sprague-Dawley rats (male, 180-200 g) aged 8-10 weeks were provided from the Center of Comparative and Experimental Medicine at Shiraz University of Medical Sciences. The rats were housed in standard conditions in separate cages. In the beginning of

the experiment, the animals were anesthetized using an intraperitoneal injection of ketamine (5 mg/kg; Woerden, the Netherlands) and xylazine (20 mg/kg; Alfazyne, Woerden, the Netherlands) cocktail. The animals were burned by exposing 1 cm^2 on the back region to hot water for ten seconds with a plastic ring, resulting in a second-degree burn. After burning, buprenorphine (Produlab Pharma, the Netherland) was administrated subcutaneously three times daily as post-burn analgesia until the animals were sacrificed. The rats were divided into three groups of twelve rats each; group 1 received the PCL/CTS mat, group 2 received the PCL/CTS/Propolis mats, and the third group did not receive any treatment as the control group. The prepared mat played as a dermal substitute in animal models. After 3, 7, 10, and 14 days of treatment, the animals were euthanized.

Histopathological evaluations

On days 3,7, 10, and 14, histopathologic examinations were performed. In brief, after each rat was euthanized, the tissue samples were taken from the burned tissues and fixed with a 10% buffered formaldehyde solution. Then, they were embedded in paraffin. Tissue sections (5 m thick) were prepared and stained with hematoxyline and eosin (H&E) before being evaluated by a surgical pathologist, blindly under a light microscope (CX31 Model, Olympus, Japan). The existence and grade of inflammation, granulation, re-epithelialization, and angiogenesis were used for reporting histopathological scores. A score was arbitrarily dedicated (0, absent; 1, scarcely present; 2, present; 3, highly present; 4, intensively present) to each of the above-stated groups to compare them quantitatively.

Statistical analysis

All experiments were performed in triplicates, and results were expressed as mean ± standard deviation (SD). Statistical analyses were performed by GraphPad Prism version 9.0, using a one-way ANOVA test. Statistical significance was considered as $*P<0.05$, $**P<0.01$, $***P<0.001$ and $****P<0.0001$.

Results

Amount of total phenol and flavonoids contents in propolis extract

The calibration curve of gallic acid is illustrated in Fig. 1A. The total phenol content in propolis extracts stock solution was 123.34 ± 0.44 mg/L and 493.38 ± 1.77 mg/g in the propolis extract. The calibration curve of the quercetin is presented in Fig. 1B. The total flavonoid content in the propolis extracts stock solution was 32.15 ± 1.74 mg/L and 128.62 ± 6.99 mg/g in the propolis extract.

SEM evaluation of the morphology of the nanofibrous mats

SEM photography was used to assess the morphology of nanofibrous mats (Fig. 2). Proper nanofibers with a smooth, bead-free, and homogeneous structure were gained from all polymeric blends (Fig. 2). The mean fiber diameter of electrospun mats was 743.9 ± 15.6, 626.7 ± 133.7, and 589.3 ± 26.58 nm for PCL, PCL/CTS, and PCL/CTS/Propolis, respectively.

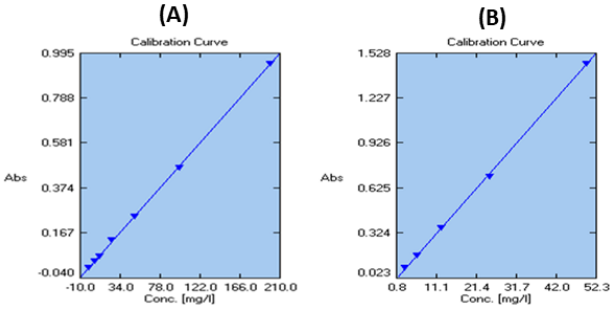

Fig. 1. Calibration curve of gallic acid (A) and quercetin (B).

The diameter of nanofibers in PCL/CTS/Propolis showed a significant decrease compared to the raw PCL mat. Also, the number of pores was significantly higher in PCL/CTS/Propolis mat in comparison to the PCL mat. No remarkable difference was observed in the three mats in terms of mean pore area as well as the percentage of porosity (Fig. 3).

Surface roughness

AFM was carried out for assessing the topographical features and Surface roughness of the fabricated mats. AFM images of PCL, PCL/CTS, and PCL/CTS/Propolis nanofibrous mats are shown in Fig. 2C, 2F, and 2I, respectively. The surface roughness in PCL, PCL/CTS, and PCL/CTS/Propolis nanofibrous mats was 143.49, 237.52, and 368.54 nm, respectively.

FTIR analysis of the mats

The chemical composition of the mats was investigated using FTIR analysis, and their FTIR spectrums are illustrated in Fig. 4. In the spectrum of the neat PCL mat, two peaks at 2990 and 2860 cm^{-1} are attributed to asymmetric and symmetric CH_2 stretching vibrations. A strong peak at 1724 cm^{-1} can be attributed to the stretching vibration of C═O of carbonyl groups.[24] A vibrational peak at 1292 cm^{-1} is attributed to stretching of C–O and C–C. Two peaks at 1240 and 1168 cm^{-1} are related to asymmetric and symmetric stretching of C–O–C, respectively.[25] A broad absorption band in the range of 3200–3700 cm^{-1} in the FTIR spectrum of the PCL/CTS blend is related to N–H and O–H stretching vibrations of CTS that overlap with each other. Two bands at 1684 and 1528 cm^{-1} are assigned to amide-I and amide-II of CTS.[25,26] The spectrum of PCL/CTS/Propolis exhibits a peak at 3394 cm^{-1}, which is attributed to the O–H stretching vibration of propolis phenolic groups. Peaks located at 1438 cm^{-1} and 1260 cm^{-1} correspond to stretching vibration of the C–H and C–O groups of polyols, e.g. hydroxy flavonoids of the propolis extract.[27] A peak at 1376 cm^{-1} is probably

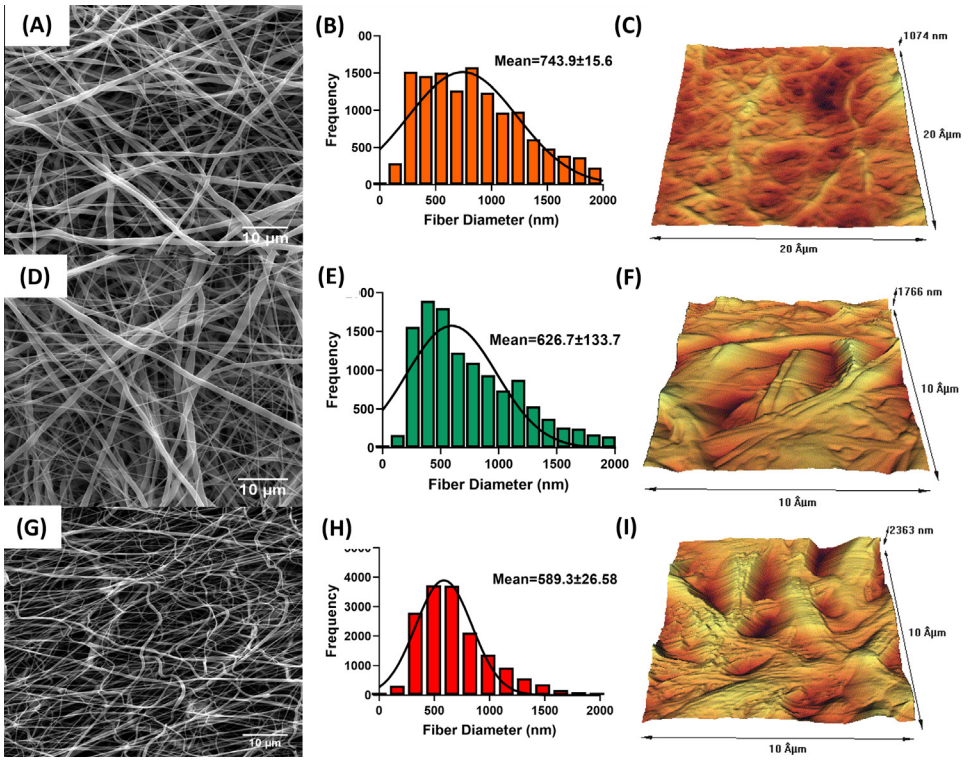

Fig. 2. SEM photomicrograph, fiber diameter frequency, and AFM images of the surface of electrospun PCL (A-C), PCL/CTS (D-F), and PCL/CTS/Propolis (G-I) nanofibrous mats, respectively.

assigned to the C–H stretching of the deformed aromatic ring.[28] Bands at 1048 and 852 cm^{-1} might correspond to stretching vibration of C–O, and C–H groups of aromatic ring vibration or to ethanol.[29,30] Some bands in the FTIR spectrum of the PCL/CTS/Propolis composite were widened and intensified compared to raw PCL and PCL/CTS blend spectrum that might be due to molecular interactions and hydrogen bonds between PCL, CTS, and propolis. Also, some minor positional deviations of peaks in FTIR spectrums of the fabricated blends could be caused by physical changes following molecular weight reduction.[31]

Mechanical properties of the mats

The amount of UTS and percentage of elongation at break are represented in Fig. 5A and B, respectively. The results indicated that the addition of CTS to the PCL led to a significant ($P < 0.001$) reduction of UTS (from 1.75 ± 0.07 to 1.26 ± 0.19 MPa) and a remarkable ($P < 0.001$) decrease in the elongation at break percent (from 113.38 ± 6.8 to 69.01 ± 9.97%, $P < 0.05$). When compared to the PCL/CTS nanofibrous mat, the addition of propolis significantly ($P < 0.05$) elevated both UTS and elongation at break parameters. The UTS and elongation at break for PCL/CTS/Propolis nanofibrous mats were at 1.85 ± 0.13 MPa and 114.03 ± 12.1%, respectively.

Contact angle of the mats

The water contact angle of the surface is a wettability

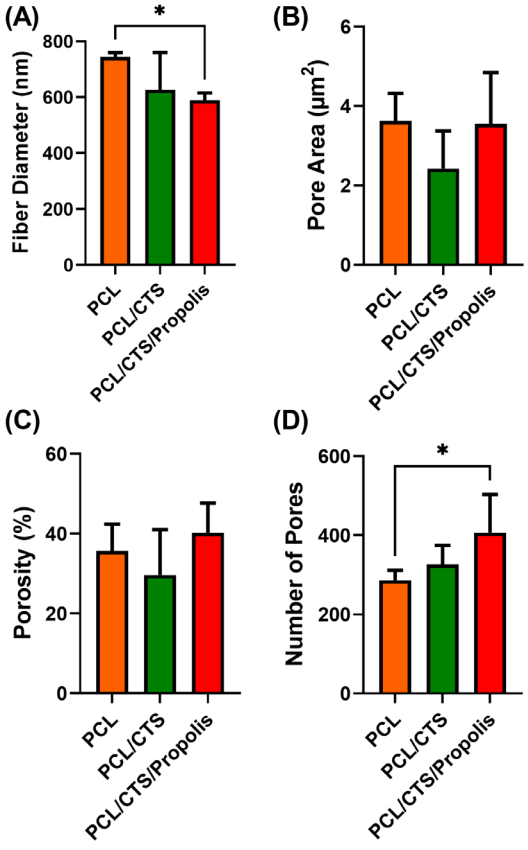

Fig. 3. DiameterJ parameters of PCL, PCL/CTS, and PCL/CTS/Propolis electrospun mats. Data are expressed as mean ± SD. *$P < 0.05$.

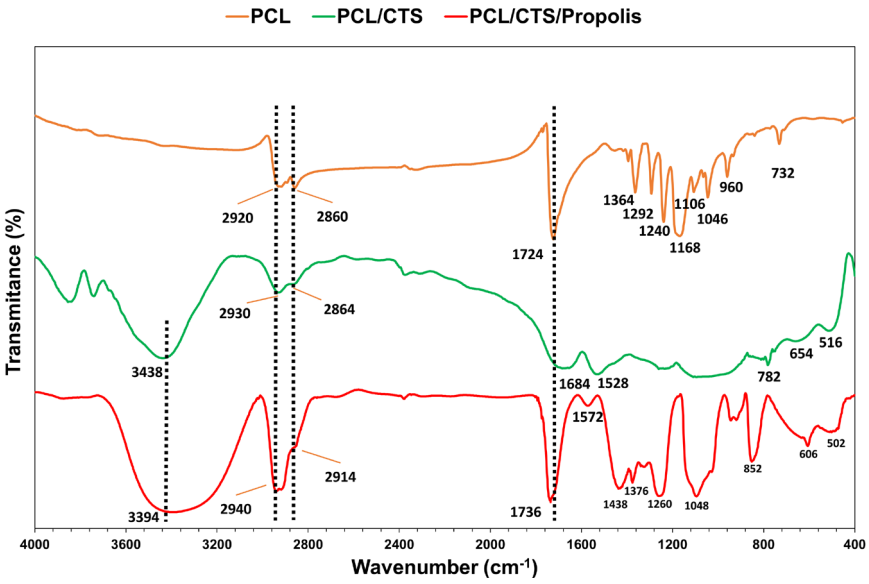

Fig. 4. FTIR spectra of PCL, PCL/CTS, and PCL/CTS/Propolis nanofibrous mats.

indicator of biomaterials.[32,33] The contact angle of the PCL, PCL/CTS, and PCL/CTS/Propolis mats was 114.5 ± 3.3°, 81.84 ± 10.16°, and 125 ± 6.44°, respectively. As illustrated in Fig. 5C, the addition of CTS to PCL significantly decreased the water contact angle compared to raw PCL. Meanwhile, mixing propolis with the PCL and CTS remarkably increased the contact angle of the fabricated electrospun mat in comparison to the PCL/CTS mat.

Swelling ratio and remaining weight of the mats

The swelling ratio was used to calculate the water absorption capability of the mats. The swelling ratio was gradually increased until it reached equilibrium after 12 hours. After 24 hours (equilibrium state), the swelling ratios for PCL, PCL/CTS, and PCL/CTS/Propolis mats were 218.4 ± 19.38, 326.54 ± 7.03, and 273.88 ± 13.54%, respectively. After 24 hours, the higher significant swelling ratio significantly belonged to PCL/CTS mat compared to the two other mats. Also, a significant increase was observed in PCL/CTS/Propolis in comparison to raw PCL electrospun mat (Fig. 5E). Fig. 5F shows the degradation profile of the nanofibrous mats. A significant weight loss was observed when the CTS as a hydrophile polymer was added to the nanofibrous composite, while the addition of the propolis by hydrophobic properties did not increase the water uptake and the degradation ratio.

Propolis release kinetic from the PCL/CTS/Propolis mat

The drug release profile of propolis from the PCL/CTS/Propolis mat is represented in Fig. 5F. About 60% of drug

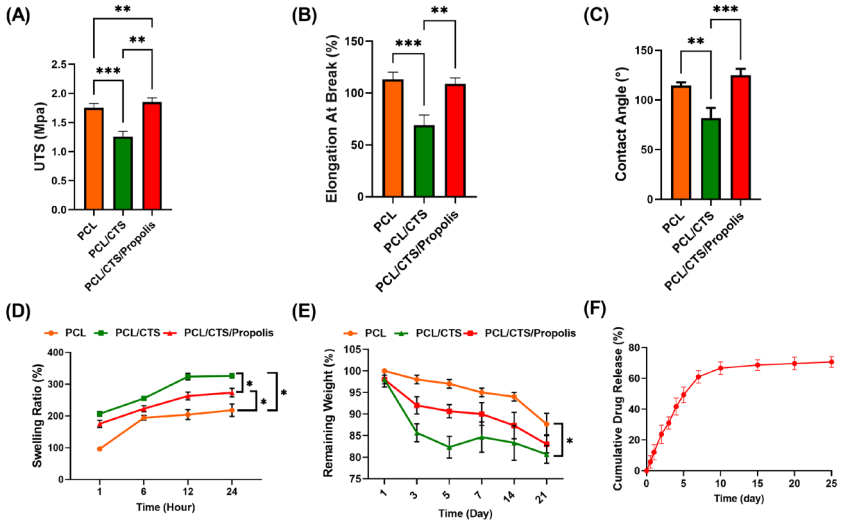

Fig. 5. (A) Tensile strength, (B) elongation at break, (C) contact angle, (D) swelling ratio, and (E) remaining weight in PCL, PCL/CTS, and PCL/CTS/Propolis nanofibrous mats, respectively. (F) Cumulative drug release profile of propolis from the PCL/CTS/Propolis scaffold (C). Data are expressed as mean ± SD. *P < 0.05, **P < 0.01, and ***P < 0. 001.

release from the PCL/CTS/Propolis mat was observed until day 7. Then, the release rate slowed down on days 7 to 10. Almost a steady sustained release was observed on days 10 to 25, and, eventually, about 70% of propolis was released.

SEM analysis of cell attachment

SEM images from electrospun mats revealed that HDFs could attach and preserve their natural shape on the fabricated PCL/CTS/Propolis mat that accentuated the biocompatibility of the mats (Fig. 6A). Based on the SEM images, it seems that a higher number of cells were attached on the PCL/CTS/Propolis mat in comparison to PCL and PCL/CTS nanofibrous mats.

DAPI staining

The biocompatibility of the mats was tested using DAPI fluorescent staining (Fig. 6B). The results showed that the number of cells on pure PCL mats was relatively low, whereas the number of cells on PCL/CTS and PCL/CTS/Propolis mats was higher.

MTT assay

The MTT assay was performed to assess the biocompatibility of the electrospun mats. When compared to the control group (culture plate), cell viability increased in all mat groups. This could be due to the nanofibrous structure of the mats, which mimics the native skin matrix as a skin substitute. CTS is known as a biocompatible natural polymer that can increase the cell attachment and proliferation. At 48 and 72 hours, the PCL/CTS ($P<0.05$) mat had significantly higher cell viability in comparison to the PCL nanofibers. Similarly, the PCL/CTS/Propolis mat showed a significant ($P<0.01$ at 48 hours and $P<0.05$ at 72 hours) increase in cell viability percentage compared to the raw PCL mat (Fig. 6C).

In vivo wound closure study

Macroscopic photographs of the wounds at PCL, PCL/CTS, and PCL/CTS/Propolis groups during time and the process of wound closure are illustrated in Fig. 7A and 7B, respectively. As shown in Fig. 7C, no significant difference in the percentage of wound closure was observed between the groups on day 3, while on the other days wound closure percentage was significantly ($P<0.05$) higher in the animal dressed with PCL/CTS and PCL/CTS/Propolis mats than in the other animals dressed with PCL nanofibers. Also, a remarkable ($P<0.00001$) difference was observed between PCL/CTS and PCL/CTS/Propolis groups on day 7.

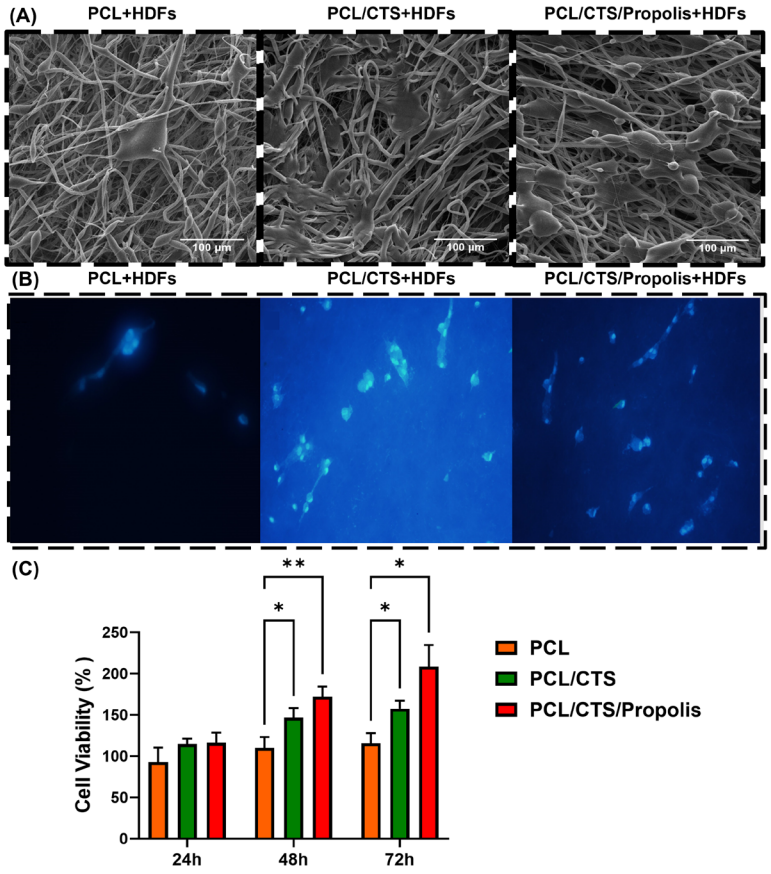

Fig. 6. (A) SEM images of HDFs attachment and proliferation on PCL, PCL/CTS, and PCL/CTS/Propolis scaffolds. (B) DAPI staining of PCL, PCL/CTS, and PCL/CTS/Propolis nanofibrous scaffolds cultured with HDFs. (C) Cell viability percent on different scaffolds after 24, 48, and 72h. Data are expressed as mean ± SD. *P<0.05, and **P<0.01.

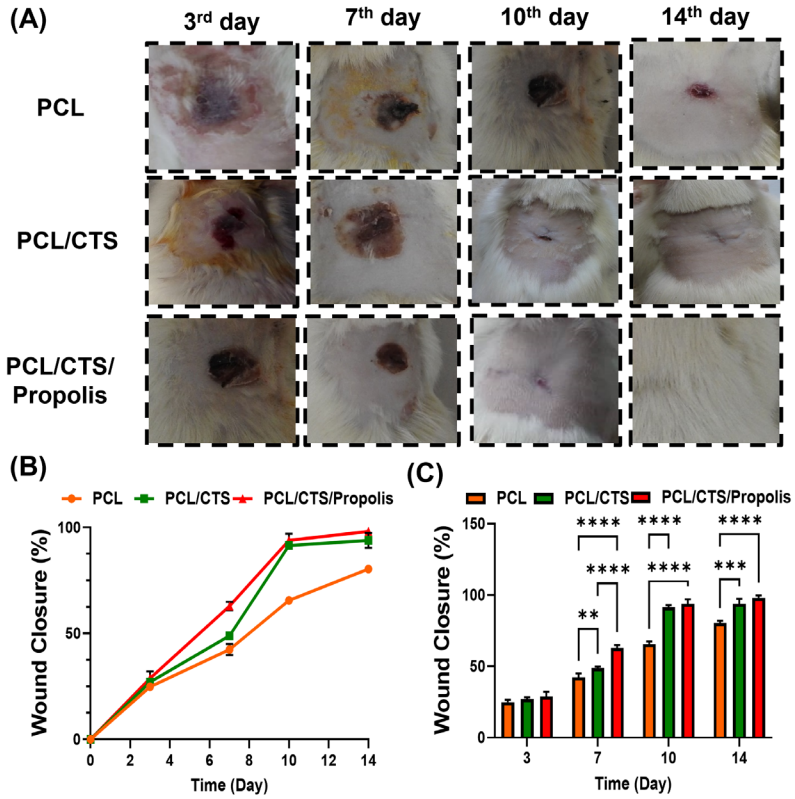

Fig. 7. (A) Macroscopic micrograph of wounds and (B) percentage of wound closure in rats dressed with PCL, PCL/CTS, and PCL/CTS/Propolis mats. Data are expressed as mean ± SD. **P*<0.05, and ***P*<0.01.

In vivo histopathological examinations

Histopathological evaluations on experimental wounds dressed with PCL, PCL/CTS, and PCL/CTS/Propolis mats were carried out to assess the wound healing capabilities of nanofibrous mats (Fig. 8A). On day 3, no significant differences were found between the groups in terms of inflammation, granulation, re-epithelialization, and angiogenesis scores. On day 7, the inflammation score was significantly decreased ($P<0.05$), while granulation and angiogenesis scores were significantly ($P<0.05$) elevated in animals dressed with the PCL/CTS/Propolis mat when compared to those dressed with PCL nanofibers. On day 10, the inflammation score was remarkably lower in PCL/CTS and PCL/CTS/Propolis groups than in the PCL group ($P<0.05$ and $P<0.01$, respectively). Also, granulation, re-epithelialization, and angiogenesis scores were significantly ($P<0.05$) higher in the PCL/CTS/Propolis group compared to the PCL group. On day 14, a significant ($P<0.05$) decrease in the inflammation score, and, on the other hand, a remarkable ($P<0.05$) increase in granulation, re-epithelialization, and angiogenesis scores was observed in the skin samples dressed with the PCL/CTS/Propolis mat in comparison to the PCL nanofibers (Fig. 8B-E).

Discussion

Morphological properties of the fabricated mats influence infiltration, proliferation, and function of cells. SEM images showed that all the fabricated electrospun mats had a fully porous structure with no bead formation. The addition of propolis to the polymeric composite resulted in a significant reduction in the fiber diameter and an increase in the number of pores in the fabricated PCL/CTS/Propolis mat compared to the neat PCL mat. The combination of new compounds can lead to determinantal changes in the viscosity of electrospinning solution, which has an important role in the process of fibers formation and modifies the spinnability and morphology of electrospun nanofibers.[34]

AFM analysis revealed that addition of CTS and propolis to PCL increased the surface roughness of the fabricated mats. The surface roughness of the electrospun mats has a key role in the attachment of the cells to the mat.[35] Higher roughness of the mat surface is associated with enhancing the attachment and spreading of the cultured cells.[35] Therefore, the increase of surface roughness in the PCL/CTS/Propolis mat may contribute to the cell adhesion.

The mechanical strength of electrospun nanofibers is considered an important factor for wound dressing.[36] Findings from the present study revealed that although the PCL/CTS mat had significantly lower UTS and percentage of elongation at break in comparison to the raw PCL mat, the addition of propolis to the PCL/CTS blend increased both mentioned parameters in the fabricated mat compared to the PCL/CTS mat. Therefore, the adhesive property of propolis could be useful to

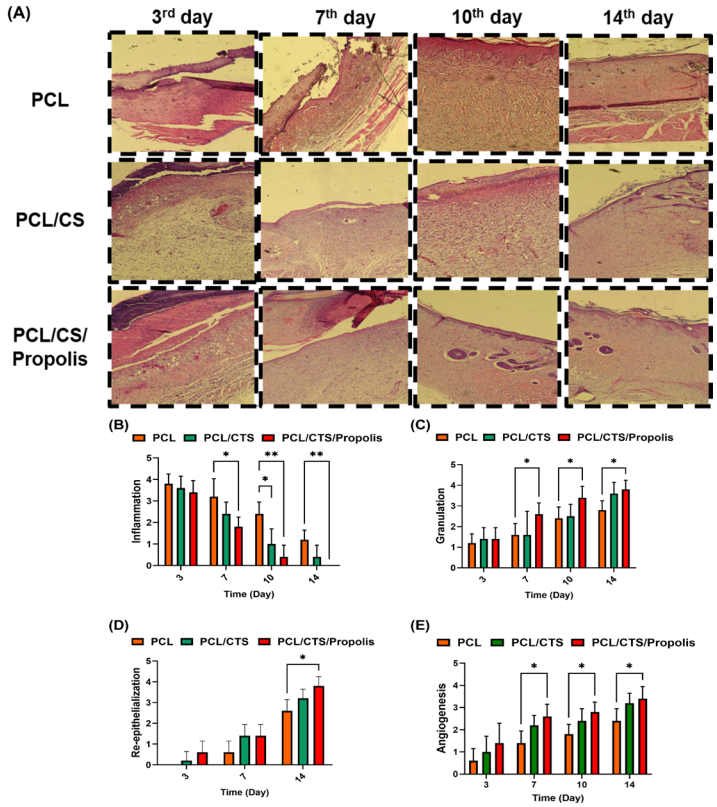

Fig. 8. (A) Photomicrographs of histological sections of wound site groups on days 3, 7, 10, and 14 obtained from burn-induced wounds from rats dressed with PCL, PCL/CTS, and PCL/CTS/Propolis nanofibrous mats. (B-E) Histopathological scores, including inflammation, granulation, re-epithelialization, and angiogenesis. *P<0.05, **P<0.01, and **P<0.01.

enhance the mechanical strength of nanocomposite fibers. Similar to our findings, Kim et al[36] have reported that the combination of propolis with polyurethane increased the mechanical strength of the electrospun fibrous mat.

Appropriate hydrophilicity is a critical parameter for wound dressing and is associated with better cell-mat interaction.[37] Hence, the hydrophilicity of the fabricated mats was evaluated using water contact angle and swelling behavior assays. Results obtained from the water contact angle assay indicated that PCL/CTS had significantly more surface wettability compared to raw PCL. Also, the swelling ratio was remarkably increased in PCL/CTS and PCL/CTS/Propolis mats in comparison to the raw PCL mat. The elevation of hydrophilicity in both PCL/CTS and PCL/CTS/Propolis is due to the presentation of CTS in the structure of electrospun mats.

Findings from the swelling assay showed that PCL/CTS and PCL/CTS/Propolis mats had a higher ratio of swelling than PCL nanofibers. It can lead to better diffusion of fluids into the fibrous nanocomposite and result in more release of propolis. On the other hand, cell attachment to the mat is directly related to the hydrophilic properties of the fabricated mat.[37] Therefore, the addition of CTS and propolis to PCL can help the cells to better attach and subsequently proliferate into the fabricated mat which was confirmed by the findings from the MTT assay. The results revealed that PCL/CTS/Propolis mat increased the viability and proliferation of HDFs; this indicates that this fibrous nanocomposite is nontoxic and biocompatible for use in the treatment of cutaneous wounds. propolis has good adhesive properties.[38] Therefore, it can enhance anchoring and subsequent proliferation of the cells on the fabricated mat.[36] In line with our results, Alberti et al have reported an electrospun polyvinyl alcohol (PVA) nanocomposite containing propolis-nanoparticle (NP) which was non-toxic for NIH/3T3 fibroblast cells. However, they did not find a significant difference in the percentage of cell viability between neat PVA and PVA/propolis-NPs mats.[39] Also, the MTT assay for two other polyurethane-based nanofibrous mats containing propolis showed that fabricated electrospun mats were biocompatible and non-toxic for L929 fibroblast cells which were similar to the findings of the present study.[40, 41]

The mat must be biodegradable to allow the tissue to produce its own ECM.[42] Favorable skin wound dressing scaffolds should degrade within 3-4 weeks at the wound site.[43] Among the electrospun fabricated mats in this study, the PCL/CTS nanofibrous mat significantly had a higher amount of weight loss compared to the neat PCL mat which had the lowest weight loss. These findings indicated the addition of CTS and propolis to a crystalline and hydrophobic polymer added desirable biodegradability to the fabricated mat.

It has been proven that using electrospun nanofibrous

mats is a good practical strategy for controlling the drug delivery.[44] Their high surface-to-volume ratio can cause improvement in drug loading and various bioactive molecules with different bioactivities; for example, anti-inflammatory and anti-bacterial agents are capable to encapsulate into nanofibers.[44, 45] This method is especially advantageous for enhancing the delivery of low soluble drugs.[44] Our findings indicated that electrospinning a polymeric PCL/CTS blend containing propolis provided a sustainable means for consecutive release of propolis, which is a low soluble bioactive compound. Similarly, in two other studies conducted by Eskandarnia et al, the results indicated that nanofibrous mats created by the electrospinning technique provided sustainable platforms for the continuous release of propolis.[40,41]

Macroscopical evaluations showed that grafting PCL/CTS/Propolis nanocomposite fibrous mat accelerated the percentage of wound closure in the rat models of burn-induced skin injury. In line with our results, Eskandarnia et al[41] have reported that mixing ethanolic extract of propolis with polyurethane and hyaluronic acid decreased the wound area in a rat model of the excisional wound. Similarly, in another study, Eskandarnia et al[40] revealed that a bilayer wound dressing containing ethanolic extract of propolis remarkably reduced the wound area in rats. Altogether, it seems that wound dressing grafts containing propolis accelerate the process of wound healing in experimental animal models.

Researchers believe that propolis can reduce the amount of excessive free radicals at the wound site, which impair the wound healing process.[16,46] Our findings indicated that propolis possesses Gallic acid and quercetin, which are both potent phenolic antioxidants.[46,47] Therefore, the wound healing accelerating effects of PCL/CTS/Propolis observed in this study could be due to the antioxidant activity of propolis.

On the other hand, there is some evidence of a modulatory role of propolis in promoting TGFβ/Smad signaling that up-regulates expression and deposition of collagen type I, elevates proliferation of the fibroblasts and keratinocytes, and induces angiogenesis in a cutaneous wound.[48] In line with these findings, histopathological evaluation in the present study revealed that grafting nanocomposite fibrous mat containing propolis on cutaneous wound induced by burn injury reduced inflammation and enhanced skin tissue angiogenesis, granulation, and re-epithelialization in the rat model. Hence, the accelerating effects of PCL/CTS/Propolis could also be owing to the anti-inflammatory activity of propolis.

Conclusion

In summary, the PCL/CTS/Propolis mat was successfully fabricated with appropriate morphological, physiochemical, and biological properties. PCL/CTS/Propolis mat prepared in this study had proper hydrophilicity and water uptake capacity, as well as good mechanical characteristics and a beadless nanofibrous shape. In addition, findings from the present study revealed that PCL/CTS/Propolis electrospun mat showed biocompatibility and accelerated wound healing in the rat model of burn injury.

Research Highlights

What is the current knowledge?

√ Fabricated mats composed of PCL, CTS, and natural bioactive compounds have shown promising effects in dressing skin wounds.

√ Propolis is a natural resinous compound that possesses antioxidant, anti-inflammatory, and wound healing properties.

What is new here?

√ The fabricated nanofibrous mat composed of PCL, CTS, and propolis exhibited acceptable physical, chemical, and biocompatible characteristics.

√ The PCL/CTS/Propolis mat had the potential for dressing the skin wounds.

Acknowledgment

We appreciate the Burn and Wound Healing Research Center of Shiraz University of Medical Sciences, which helped us in this project. The authors would like to thank Shiraz University of Medical Sciences, Shiraz, Iran and also Center for Development of Clinical Research of Nemazi hospital and Dr. Nasrin Shokrpour for editorial assistance.

Authors' Contribution

Conceptualization: Seyedeh-Sara Hashemi, Ali Akbar Mohammadi.
Data curation: Seyedeh-Sara Hashemi, Seyedeh-Somayeh Rajabi, Mehdi Kian.
Formal analysis: Seyedeh-Sara Hashemi, Mehdi Kian.
Funding acquisition: Seyedeh-Sara Hashemi, Ali Akbar Mohammadi, Zahra Zarei.
Investigation: Seyedeh-Somayeh Rajabi, Alireza Rafati, Mehdi Kian.
Methodology: Seyedeh-Sara Hashemi, Seyedeh-Somayeh Rajabi, Mehdi Kian.
Project administration: Seyedeh-Sara Hashemi, Ali Akbar Mohammadi, Zahra Zarei.
Resources: Seyedeh-Sara Hashemi, Zahra Zarei.
Supervision: Ali Akbar Mohammadi, Zahra Zarei.
Validation: Seyedeh-Sara Hashemi, Ali Akbar Mohammadi.
Visualization: Seyedeh-Sara Hashemi, Parisa Sanati, Mehdi Kian.
Writing–original draft: Seyedeh-Sara Hashemi, Parisa Sanati, Mehdi Kian.
Writing–review editing: Seyedeh-Sara Hashemi, Mehdi Kian.

Competing Interests

Authors declare all relevant interests that could be perceived as conflicting.

Data Availability Statement

Respectful readers may contact the corresponding author to reach all the data.

Ethical Statement

All the tests were carried out under the rules and regulations of the Iran Veterinary Organization for working with laboratory animals. The study protocol was approved by the ethics committee of Shiraz University of Medical Sciences (Code: IR.SUMS.REC. 1395.S716).

Funding
None.

References

1. Bacakova L, Zikmundova M, Pajorova J, Broz A, Filova E, Blanquer A, et al. Nanofibrous scaffolds for skin tissue engineering and wound healing based on synthetic polymers. In: *Applications of Nanobiotechnology.* IntechOpen; 2020. https://doi.org/10.5772/intechopen.88744
2. Howard D, Buttery LD, Shakesheff KM, Roberts SJ. Tissue engineering: strategies, stem cells and scaffolds. *J Anat* **2008**; 213: 66-72. https://doi.org/10.1111/j.1469-7580.2008.00878.x
3. Pilehvar-Soltanahmadi Y, Akbarzadeh A, Moazzez-Lalaklo N, Zarghami N. An update on clinical applications of electrospun nanofibers for skin bioengineering. *Artif Cells Nanomed Biotechnol* **2016**; 44: 1350-64. https://doi.org/10.3109/21691401.2015.1036999
4. Homaeigohar S, Boccaccini AR. Antibacterial biohybrid nanofibers for wound dressings. *Acta Biomater* **2020**; 107: 25-49. https://doi.org/10.1016/j.actbio.2020.02.022
5. Augustine R, Dominic EA, Reju I, Kaimal B, Kalarikkal N, Thomas S. Electrospun poly(epsilon-caprolactone)-based skin substitutes: In vivo evaluation of wound healing and the mechanism of cell proliferation. *J Biomed Mater Res B Appl Biomater* **2015**; 103: 1445-54. https://doi.org/10.1002/jbm.b.33325
6. Mohamed RM, Yusoh K. A Review on the Recent Research of Polycaprolactone (PCL). *Adv Mat Res* **2015**; 1134: 249-55. https://doi.org/10.4028/www.scientific.net/AMR.1134.249
7. Mandal P, Shunmugam R. Polycaprolactone: a biodegradable polymer with its application in the field of self-assembly study. *J Macromol Sci A* **2020**; 58: 111-29. https://doi.org/10.1080/10601325.2020.1831392
8. Sahariah P, Masson M. Antimicrobial Chitosan and Chitosan Derivatives: A Review of the Structure-Activity Relationship. *Biomacromolecules* **2017**; 18: 3846-68. https://doi.org/10.1021/acs.biomac.7b01058
9. Shukla SK, Mishra AK, Arotiba OA, Mamba BB. Chitosan-based nanomaterials: a state-of-the-art review. *Int J Biol Macromol* **2013**; 59: 46-58. https://doi.org/10.1016/j.ijbiomac.2013.04.043
10. Parhi R. Drug delivery applications of chitin and chitosan: a review. *Environ Chem Lett* **2020**; 18: 577-94. https://doi.org/10.1007/s10311-020-00963-5
11. Aidun A, Safaei Firoozabady A, Moharrami M, Ahmadi A, Haghighipour N, Bonakdar S, *et al.* Graphene oxide incorporated polycaprolactone/chitosan/collagen electrospun scaffold: Enhanced osteogenic properties for bone tissue engineering. *Artif Organs* **2019**; 43: E264-E81. https://doi.org/10.1111/aor.13474
12. Fadaie M, Mirzaei E. Nanofibrillated chitosan/polycaprolactone bionanocomposite scaffold with improved tensile strength and cellular behavior. *Nanomed J* **2018**; 5: 77-89. https://doi.org/10.22038/NMJ.2018.005.004
13. Hashemi SS, Saadatjo Z, Mahmoudi R, Delaviz H, Bardania H, Rajabi SS, *et al.* Preparation and evaluation of polycaprolactone/chitosan/Jaft biocompatible nanofibers as a burn wound dressing. *Burns* **2021**. https://doi.org/10.1016/j.burns.2021.12.009
14. Anjum SI, Ullah A, Khan KA, Attaullah M, Khan H, Ali H, *et al.* Composition and functional properties of propolis (bee glue): A review. *Saudi J Biol Sci* **2019**; 26: 1695-703. https://doi.org/10.1016/j.sjbs.2018.08.013
15. Oryan A, Alemzadeh E, Moshiri A. Potential role of propolis in wound healing: Biological properties and therapeutic activities. *Biomed Pharmacother* **2018**; 98: 469-83. https://doi.org/10.1016/j.biopha.2017.12.069
16. Martinotti S, Ranzato E. Propolis: a new frontier for wound healing? *Burns Trauma* **2015**; 3: 9. https://doi.org/10.1186/s41038-015-0010-z
17. Zabaiou N, Fouache A, Trousson A, Baron S, Zellagui A, Lahouel M, *et al.* Biological properties of propolis extracts: Something new from an ancient product. *Chem Phys Lipids* **2017**; 207: 214-22. https://doi.org/10.1016/j.chemphyslip.2017.04.005
18. Sehn E, Hernandes L, Franco SL, Goncalves CC, Baesso ML. Dynamics of reepithelialisation and penetration rate of a bee propolis formulation during cutaneous wounds healing. *Anal Chim Acta* **2009**; 635: 115-20. https://doi.org/10.1016/j.aca.2009.01.019
19. Olczyk P, Komosinska-Vassev K, Winsz-Szczotka K, Stojko J, Klimek K, Kozma EM. Propolis induces chondroitin/dermatan sulphate and hyaluronic Acid accumulation in the skin of burned wound. *Evid Based Complement Alternat Med* **2013**; 2013: 290675. https://doi.org/10.1155/2013/290675
20. Olczyk P, Wisowski G, Komosinska-Vassev K, Stojko J, Klimek K, Olczyk M, *et al.* Propolis Modifies Collagen Types I and III Accumulation in the Matrix of Burnt Tissue. *Evid Based Complement Alternat Med* **2013**; 2013: 423809. https://doi.org/10.1155/2013/423809
21. Escriche I, Juan-Borras M. Standardizing the analysis of phenolic profile in propolis. *Food Res Int* **2018**; 106: 834-41. https://doi.org/10.1016/j.foodres.2018.01.055
22. Chang CC, Yang MH, Wen HM, Chern JC. Estimation of total flavonoid content in propolis by two complementary colometric methods. *J Food Drug Anal* **2020**; 10. https://doi.org/10.38212/2224-6614.2748
23. Hotaling NA, Bharti K, Kriel H, Simon CG, Jr. DiameterJ: A validated open source nanofiber diameter measurement tool. *Biomaterials* **2015**; 61: 327-38. https://doi.org/10.1016/j.biomaterials.2015.05.015
24. Jana S, Leung M, Chang J, Zhang M. Effect of nano- and micro-scale topological features on alignment of muscle cells and commitment of myogenic differentiation. *Biofabrication* **2014**; 6: 035012. https://doi.org/10.1088/1758-5082/6/3/035012
25. Gautam S, Chou C-F, Dinda AK, Potdar PD, Mishra NC. Fabrication and characterization of PCL/gelatin/chitosan ternary nanofibrous composite scaffold for tissue engineering applications. *J Mater Sci* **2013**; 49: 1076-89. https://doi.org/10.1007/s10853-013-7785-8
26. Georgopoulou A, Kaliva M, Vamvakaki M, Chatzinikolaidou M. Osteogenic Potential of Pre-Osteoblastic Cells on a Chitosan-graft-Polycaprolactone Copolymer. *Materials (Basel)* **2018**; 11: 490. https://doi.org/10.3390/ma11040490
27. Franca JR, De Luca MP, Ribeiro TG, Castilho RO, Moreira AN, Santos VR, *et al.* Propolis--based chitosan varnish: drug delivery, controlled release and antimicrobial activity against oral pathogen bacteria. *BMC Complement Altern Med* **2014**; 14: 478. https://doi.org/10.1186/1472-6882-14-478
28. Hussein UK, Hassan NEY, Elhalwagy MEA, Zaki AR, Abubakr HO, Nagulapalli Venkata KC, *et al.* Ginger and Propolis Exert Neuroprotective Effects against Monosodium Glutamate-Induced Neurotoxicity in Rats. *Molecules* **2017**; 22: 1928. https://doi.org/10.3390/molecules22111928
29. Oliveira RN, Mancini MC, Oliveira FCSd, Passos TM, Quilty B, Thiré RMdSM, *et al.* FTIR analysis and quantification of phenols and flavonoids of five commercially available plants extracts used in wound healing. *Matéria (Rio de Janeiro)* **2016**; 21: 767-79. https://doi.org/10.1590/S1517-707620160003.0072
30. Mudalip SKA, Bakar MRA, Adam F, Jamal P. Structures and Hydrogen Bonding Recognition of Mefenamic Acid Form I Crystals in Mefenamic Acid/ Ethanol Solution. *Int J Chem Eng* **2013**; 4: 124-8. https://doi.org/10.7763/ijcea.2013.V4.277
31. Roozbahani F, Sultana N, Fauzi Ismail A, Nouparvar H. Effects of Chitosan Alkali Pretreatment on the Preparation of Electrospun PCL/Chitosan Blend Nanofibrous Scaffolds for Tissue Engineering Application. *J Nanomater* **2013**; 2013: 1-6. https://doi.org/10.1155/2013/641502
32. Agrawal G, Negi YS, Pradhan S, Dash M, Samal SK. Wettability and contact angle of polymeric biomaterials. In: *Characterization of Polymeric Biomaterials*. Elsevier; **2017**. p. 57-81. https://doi.org/10.1016/b978-0-08-100737-2.00003-0
33. Raja IS, Lee SH, Kang MS, Hyon S-H, Selvaraj AR, Prabakar K, *et al.* The predominant factor influencing cellular behavior

on electrospun nanofibrous scaffolds: Wettability or surface morphology? *Mater Des* **2022**; 216: 110580. https://doi.org/10.1016/j.matdes.2022.110580
34. Persano L, Camposeo A, Tekmen C, Pisignano D. Industrial Upscaling of Electrospinning and Applications of Polymer Nanofibers: A Review. *Macromol Mater Eng* **2013**; 298: 504-20. https://doi.org/10.1002/mame.201200290
35. Chung T-W, Liu D-Z, Wang S-Y, Wang S-S. Enhancement of the growth of human endothelial cells by surface roughness at nanometer scale. *Biomaterials* **2003**; 24: 4655-61. https://doi.org/10.1016/s0142-9612(03)00361-2
36. Kim JI, Pant HR, Sim HJ, Lee KM, Kim CS. Electrospun propolis/polyurethane composite nanofibers for biomedical applications. *Mater Sci Eng C Mater Biol Appl* **2014**; 44: 52-7. https://doi.org/10.1016/j.msec.2014.07.062
37. Niemczyk-Soczynska B, Gradys A, Sajkiewicz P. Hydrophilic Surface Functionalization of Electrospun Nanofibrous Scaffolds in Tissue Engineering. *Polymers (Basel)* **2020**; 12: 2636. https://doi.org/10.3390/polym12112636
38. Saccardi L, Schiebl J, Weber K, Schwarz O, Gorb S, Kovalev A. Adhesive Behavior of Propolis on Different Substrates. *Front Mech Eng* **2021**; 7: NA-NA. https://doi.org/10.3389/fmech.2021.660517
39. Alberti TB, Coelho DS, de Prá M, Maraschin M, Veleirinho B. Electrospun PVA nanoscaffolds associated with propolis nanoparticles with wound healing activity. *J Mater Sci* **2020**; 55: 9712-27. https://doi.org/10.1007/s10853-020-04502-z
40. Eskandarinia A, Kefayat A, Agheb M, Rafienia M, Amini Baghbadorani M, Navid S*, et al.* A Novel Bilayer Wound Dressing Composed of a Dense Polyurethane/Propolis Membrane and a Biodegradable Polycaprolactone/Gelatin Nanofibrous Scaffold. *Sci Rep* **2020**; 10: 3063. https://doi.org/10.1038/s41598-020-59931-2
41. Eskandarinia A, Kefayat A, Gharakhloo M, Agheb M, Khodabakhshi D, Khorshidi M*, et al.* A propolis enriched polyurethane-hyaluronic acid nanofibrous wound dressing with remarkable antibacterial and wound healing activities. *Int J Biol Macromol* **2020**; 149: 467-76. https://doi.org/10.1016/j.ijbiomac.2020.01.255
42. O'Brien FJ. Biomaterials & scaffolds for tissue engineering. *Materials Today* **2011**; 14: 88-95. https://doi.org/10.1016/s1369-7021(11)70058-x
43. Bahadoran M, Shamloo A, Nokoorani YD. Development of a polyvinyl alcohol/sodium alginate hydrogel-based scaffold incorporating bFGF-encapsulated microspheres for accelerated wound healing. *Sci Rep* **2020**; 10: 7342. https://doi.org/10.1038/s41598-020-64480-9
44. Torres-Martínez EJ, Cornejo Bravo JM, Serrano Medina A, Pérez González GL, Villarreal Gómez LJ. A summary of electrospun nanofibers as drug delivery system: Drugs loaded and biopolymers used as matrices. *Curr Drug Deliv* **2018**; 15: 1360-74. https://doi.org/10.2174/1567201815666180723114326
45. Hu J, Prabhakaran MP, Tian L, Ding X, Ramakrishna S. Drug-loaded emulsion electrospun nanofibers: Characterization, drug release and in vitro biocompatibility. *RSC Adv* **2015**; 5: 100256-67. https://doi.org/10.1039/C5RA18535A
46. Salehi B, Machin L, Monzote L, Sharifi-Rad J, Ezzat SM, Salem MA*, et al.* Therapeutic Potential of Quercetin: New Insights and Perspectives for Human Health. *ACS Omega* **2020**; 5: 11849-72. https://doi.org/10.1021/acsomega.0c01818
47. Kahkeshani N, Farzaei F, Fotouhi M, Alavi SS, Bahramsoltani R, Naseri R*, et al.* Pharmacological effects of gallic acid in health and diseases: A mechanistic review. *Iran J Basic Med Sci* **2019**; 22: 225-37. https://doi.org/10.22038/ijbms.2019.32806.7897
48. Hozzein WN, Badr G, Al Ghamdi AA, Sayed A, Al-Waili NS, Garraud O. Topical application of propolis enhances cutaneous wound healing by promoting TGF-beta/Smad-mediated collagen production in a streptozotocin-induced type I diabetic mouse model. *Cell Physiol Biochem* **2015**; 37: 940-54. https://doi.org/10.1159/000430221
.94